Development of nanoparticle-filled polypropylene-based single polymer composite foams

Görbe Á., Varga L. J., Bárány T.

Accepted for publication in Heliyon
Published in 2023
DOI: 10.1016/j.heliyon.2023.e19638

Heliyon 9 (2023) e19638

Contents lists available at ScienceDirect

Heliyon

journal homepage: www.cell.com/heliyon

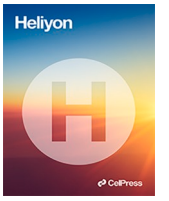

Development of nanoparticle-filled polypropylene-based single polymer composite foams

Ákos Görbe [a], László József Varga [a], Tamás Bárány [a,b,*]

[a] Department of Polymer Engineering, Faculty of Mechanical Engineering, Budapest University of Technology and Economics, Műegyetem rkp. 3., H-1111 Budapest, Hungary
[b] MTA-BME Lendület Lightweight Polymer Composites Research Group, Műegyetem rkp. 3., H-1111 Budapest, Hungary

ARTICLE INFO

Keywords:
Single polymer composites (SPC)
Nanocomposites
Foaming
Mechanical properties
Impact properties

ABSTRACT

In this study, our focus was on developing and investigating nanoparticle-filled polypropylene-based single polymer composite foams. These composites had porous and nanotube-reinforced matrices, with plain woven polypropylene (PP) fabric as reinforcement. Our main objective was to enhance the energy absorption and stiffness of the single polymer composites (SPCs) by modifying their matrices. We produced SPCs with two different matrices: one of amorphous poly-alpha-olefin (APAO) and one of thermoplastic elastomer (TPE) blended with APAO. We observed that the APAO matrix exhibited better impregnation of the fabric due to its low viscosity, while the composites with the TPE matrix showed significantly better tensile properties. The foaming process applied to the matrices resulted in a substantial increase in energy absorption for the SPCs, while preserving their tensile properties relative to their density. Scanning electron microscope images confirmed that foaming of the APAO matrix was notably more effective, primarily due to its low viscosity. Furthermore, we successfully enhanced the stiffness and tensile properties of the SPCs by nano-reinforcing the matrices with multi-wall carbon nanotubes (MWCNTs). Due to the size of the nanotubes, this reinforcement did not compromise the impact properties of the SPCs. Scanning electron microscope images also demonstrated improved dispersion of the nanotubes within the APAO matrices.

1. Introduction

Nowadays, the use of polymers for technical applications is becoming more and more widespread. Since polymers have a low density, they can be used to produce lightweight components. Weight reduction is an essential part of producing more environmentally friendly vehicles—it reduces their emission and ecological footprint [1]. However, the tensile properties of polymeric materials are well short of those of other structural materials. Therefore, it is common to use carbon or glass reinforcement for enhanced stiffness and strength at the cost of reduced impact properties and recyclability, or use biodegradable reinforcement to produce biocomposites [2].

Single polymer composites (SPCs) are polymeric composites where both the matrix and the reinforcement are of the same polymer family, most commonly polypropylene (PP) [3]. The main advantage of SPCs is that they are fully thermoplastic, thus fully recyclable by remelting [4]. The reinforcement is built up by highly oriented tapes, which grants the composite enhanced tensile properties, while

* Corresponding author. Department of Polymer Engineering, Faculty of Mechanical Engineering, Budapest University of Technology and Economics, Műegyetem rkp. 3., H-1111 Budapest, Hungary.
E-mail address: barany@pt.bme.hu (T. Bárány).

https://doi.org/10.1016/j.heliyon.2023.e19638
Received 17 May 2023; Received in revised form 29 August 2023; Accepted 29 August 2023
Available online 4 September 2023

the thermoplastic matrix provides outstanding impact properties. The most common ways to produce SPCs are hot compaction [5,6], consolidation of coextruded tapes [7], and film stacking [8,9]. A major difficulty in manufacturing single polymer composites is the narrow processing window of temperature: if the temperature is too low, the matrix does not melt; if it is too high, the reinforcement also melts or relaxes (which leads to weaker tensile properties) [10]. This processing window can be widened by exploiting crystalline polymorphism [11]; or using materials with a low melting temperature as the matrix, such as certain polypropylene-based thermoplastic elastomers [12]. Amorphous poly-alpha-olefins (APAO) exhibit an intriguing potential as matrix materials for PP-based SPCs. These materials are characterized by a predominantly atactic arrangement of propylene repeating units, similar to atactic PP, with a low melting temperature. As such, APAO can be effectively utilized as the matrix component in SPCs, offering advantageous properties for their overall performance [13]. The consolidation quality of SPCs is a critical property that directly impacts their void content and, consequently, their tensile properties. Improved consolidation quality leads to fewer microvoids, reducing their weakening effect on the composites [14].

One of the advantages of SPCs is their enhanced impact properties. Compared to fiber-reinforced polymer composites, SPCs tend to absorb much more energy upon impact due to the polymeric reinforcement [15]. The absorbed energy depends on the consolidation quality; the better consolidation is, the less energy is absorbed. The reason for this is that poorer consolidation allows for delamination and yarn pull-out at failure. This type of failure absorbs more energy than any other type associated with better consolidation. Moreover, with poor consolidation, failure is not concentrated on the point of impact, and that can also increase absorbed energy [16].

Thermoplastic elastomers (TPE) have been investigated before as matrices of SPCs. The main advantage of TPEs is that they possess elastomer-like attributes, but they can be melted; thus, they can be processed via conventional means thanks to their molecular structure. They consist of two phases: a soft elastomer phase and a hard semicrystalline thermoplastic phase. The soft phase is responsible for the rubber-like behavior and the hard phase is responsible for the thermoplastic behavior [17,18]. TPEs are manufactured in a number of different ways. Copolymerization, with block copolymers is the most widely used method. Depending on the type of the thermoplastic segment, many types of TPEs are used, for example, polyolefin-based TPEs [19]. With their polyolefin segment providing a reliable connection to the reinforcement, these materials can effectively function as the matrix in an SPC. The presence of a polyolefinic segment further enhances their suitability for serving as the matrix of a PP-based SPC [12,20].

In this paper, we present a way of enhancing the tensile properties and reducing the density of SPCs by foaming the matrix. Foams contain statistically distributed gas bubbles, which create voids in the material, thus lowering its density [21–23]. Foams are used for their low density and excellent impact resistance [24–26]. Polymer foams can be categorized by the blowing agent used in the process: there are foams made with physical (where the gas itself or a low boiling point liquid is injected into the melt) and chemical (where the the necessary gases are the byproduct of a chemical reaction) blowing agents. An innovative, new way for foaming is using thermally expandable microspheres: they consist of a thin thermoplastic layer housing a hydrocarbon that expands if heated above the boiling point, thus creating spherical cavities in the matrix [27,28]. Foaming thermoplastic elastomers is an innovative way of replacing conventional rubber foams especially in the field of shoes and sports equipment [29,30].

One obstacle to using SPCs is their low stiffness compared to fiber-reinforced composites with a thermoset matrix, caused mainly by the thermoplastic matrix of SPCs. In this article, we suggest using multi-wall carbon nanotubes (MWCNT) to strengthen the matrix so that the composites do not lose their good impact properties. The main requirement of producing nanocomposites is to achieve sufficient dispersion of the nanofillers; otherwise, they will weaken the material as aggregates [31–34]. Nanotube-filled polypropylene materials are becoming widespread, as the easy processing of PP helps create nanocomposites [35]. PP-nanocomposites are most commonly manufactured with the melt mixing method [36]. During melt mixing, the PP is melted in a processing machine (e.g., in a twin-screw extruder or an internal mixer), and the nanotubes are evenly distributed due to shear forces. PP-based CNT masterbatches are also commonly used to produce the desired homogeneity [37]. Several innovative methods have been published to make more homogeneous nanocomposites: using PP with a lower melt viscosity [38], or using a sonotrode inside an extruder [39]. Nanocomposite polymer foams are also used in innovative applications, for example, to manufacture lightweight, conductive polymeric materials with the strength ensured by the nanoparticles and the low density provided by the porous structure [40–42].

Our objective in this study was to enhance the impact properties and reduce the density of PP SPCs by foaming their matrices while maintaining their mechanical properties at the specified density. Additionally, we aimed to improve the mechanical properties of PP SPCs by reinforcing their matrices with carbon nanotubes, thereby expanding their range of applications.

2. Experimental

2.1. Materials and their processing

We used plain woven fabric composed of highly stretched split PP tapes (Tiszatextil Kft., Tiszaújváros, Hungary) as the reinforcement of the composites. The areal density of the fabric is 200 g/m^2, the tensile strength of the tapes is 421 ± 27 MPa, and their melting temperature is 168.6 °C (as determined by DSC).

Two types of materials were used as matrix for the composites: an amorphous poly-alpha-olefin–based (APAO) melt adhesive called Vestoplast® 792 (Evonik Industries AG, Essen, Germany, with a melt viscosity of 120 ± 30 Pa s at 190 °C), and an ethylene-propylene plastomer called Versify® 2000 (Dow Inc., Midland, Michigan, United States, with an MFR of 2.0 g/10 min at 230 °C with 2.16 kg). To increase the flowability of Versify 2000 we compounded it with Vestoplast® 703-type APAO (Evonik Industries AG, Essen, Germany) in a ratio of 75/25 wt% (Versify 2000/Vestoplast 703).

The matrices were foamed with 4 wt% expandable microspheres (EMS, Tracel MB 610H (Tramaco GmbH, Tornesch, Germany)). A masterbatch containing 12 wt% EMS was produced with a Labtech Engineering LTE 26–44 co-rotating twin-screw extruder (Labtech

Engineering, Samutprakarn, Thailand), and then the EMS content was reduced to 4 wt% by compounding it with neat APAO and TPE in the same extruder. The extruder was heated to 100 °C in the case of the Vestoplast 792 (referred to as APAO) matrix and 125 °C for the Versify 2000/Vestoplast 703 (referred to as TPE) so that the EMS would remain unexpanded.

We used multi-walled carbon nanotubes (MWCNT) in a concentration of 0.5 wt%, to reinforce the matrices. The type of the MWCNT used was Nanocyl NC7000 (Nanocyl SA, Sambreville, Belgium). The length of the nanotubes was 0,1–10 μm; their diameter was 10 nm, and the specific surface area was 250–300 g/m^2 (data provided by the manufacturer). To ensure proper homogeneity of the MWCNT, we produced a masterbatch with an MWCNT content of 5 wt%, using a Brabender Plasti-Corder internal mixer (Brabender GmbH & Co. KG, Duisburg, Germany) equipped with a roller-type rotor. Approximately 90% of chamber volume was filled. The masterbatch was mixed with additional matrix material using a twin-screw extruder to achieve the desired concentration. The APAO masterbatch was produced at 80 °C, and the TPE masterbatch at 120 °C. The EMS was also added to the mixture in the form of the aforementioned 12 wt% EMS masterbatch, and EMS content was also reduced to 4 wt% during compaunding. The processing temperature was 100 °C for the APAO and 125 °C for the TPE compound. A polypropylene-based (TIPPLEN H681F, MOL Petrolkémia Zrt., Tiszaújváros, Hungary, with an MFR of 1.7 g/10 min at 230 °C with 2.16 kg) CNT masterbatch was also produced with the same parameters and examined as a reference at 190 °C. Table 1 contains the components of the compounds that we used as the matrix of the composites, along with their codes.

2.2. Preparation of composites

2.2.1. Fabric coating

The composites were made by film stacking, where the matrix is sandwiched between the reinforcing fabrics as extruded sheets, then this pre-product is consolidated by the applied heat and pressure. However, the low viscosity of APAO makes standard processing difficult. Thus, special fabric-conveying equipment (Fig. 1) was used to extrude the matrix directly onto one side of the fabric. This equipment was designed and built earlier and used to develope SPCs with APAO matrices [10]. The processing temperature was 100 °C, and processing was carried out on a Labtech LCR 300 cast film–extrusion line and a Labtech 25–30/C extruder (Labtech Engineering, Samutprakarn, Thailand).

Processing the TPE-based compounds was much easier; we used traditional flat film extrusion at 125 °C on the same equipment we used with the APAO compounds.

2.2.2. Preparation of composites

Two layers of coated and one layer of uncoated fabrics were placed on each other as the pre-product of the APAO composites, and the laminates was consolidated in a Collin Teach-Line Platen Press 200 E hydraulic press (Dr. Collin GmbH, Munich, Germany) at 120 °C and 4 MPa. The preparation of Versify-based composites was similar, matrix films were put between the fabrics, then this pre-product consisting of 2 matrix and 3 reinforcement layers was consolidated in the press at 120 °C. Table 2 shows the fiber content of the composites and their relaxation measured in two perpendicular directions after consolidation.

2.3. Matrix foaming

The matrices were foamed in the hydraulic press at 135 °C for 20 min. To prevent the relaxation of the reinforcement and to guide the direction of the foaming, a frame was used on the composite to clamp it (Fig. 2). A pressure of 4 MPa was applied to the frame, which had twice the thickness of the composite; this way, foaming occurred vertically. The flowcharts in Fig. 3 shows the steps of the manufacturing process.

2.4. Characterization methods

The density of the matrices and composites was determined by a Sartorius Quintix (Sartorius, Göttingen, Germany) in distilled water at room temperature on 20 mm × 20 mm specimens according to ISO 1183. The specimen was weighed in both air and in distilled water, and the density was determined according to equation (1):

Table 1
The different codes used in the article and their meanings.

Compound	Components of the compounds
APAO	100 wt% Vestoplast 792
APAO foamed	96 wt% Vestoplast 792 + 4.0 wt% Tracel MB 610H
APAO/CNT	99.5 wt% Vestoplast 792 + 0.5 wt% MWCNT
APAO/CNT foamed	95.5 wt% Vestoplast 792 + 0.5 wt% MWCNT +4.0 wt% Tracel MB 610H
TPE	75.0 wt% Versify 2000 + 25.0 wt% Vestoplast 703
TPE foamed	71.0 wt% Versify 2000 + 25.0 wt% Vestoplast 703 + 4.0 wt% Tracel MB 610H
TPE/CNT	74.5 wt% Versify 2000 + 25.0 wt% Vestoplast 703 + 0.5 wt% MWCNT
TPE/CNT foamed	70.5 wt% Versify 2000 + 25.0 wt% Vestoplast 703 + 0.5 wt% MWCNT +4.0 wt% Tracel MB 610H

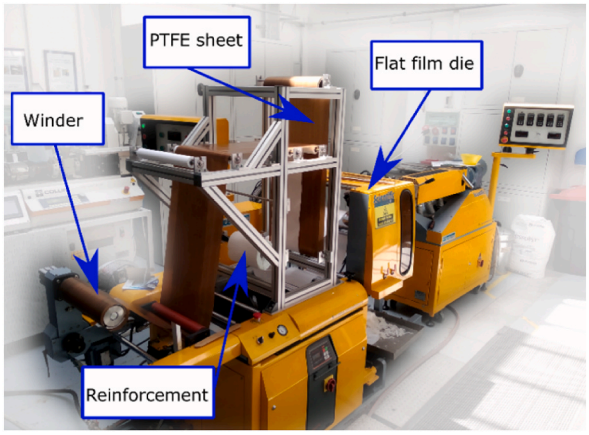

Fig. 1. The fabric coating apparatus.

Table 2
The fiber content of the prepared composites and the extent of their relaxation in warp and weft directions.

Composites	Matrix	Fiber content (%)	Relaxation (%)	
			Warp	Weft
SPC_APAO	APAO	46.5 ± 1.2	0.75 ± 0.35	1.00 ± 0.01
SPC_APAO/CNT	APAO/CNT	41.4 ± 1.9	0.87 ± 0.17	1.25 ± 0.34
SPC_TPE	TPE	40.2 ± 0.5	0.74 ± 0.33	1.01 ± 0.03
SPC_TPE/CNT	TPE/CNT	40.2 ± 0.6	0.76 ± 0.36	1.29 ± 0.37

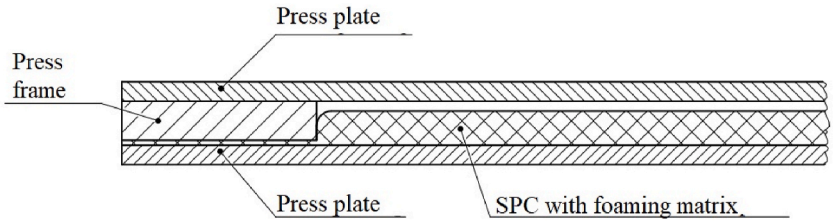

Fig. 2. The layout of matrix foaming.

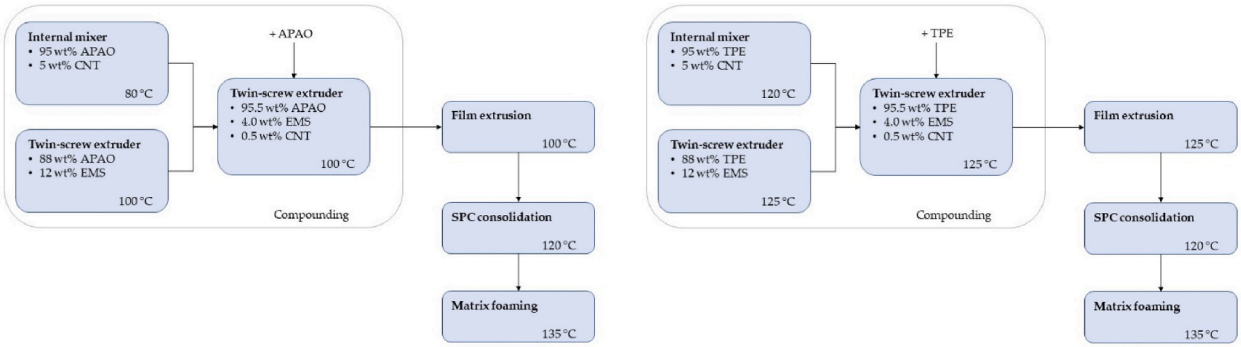

Fig. 3. Flowchart of the manufacturing process (a. SPC_APAO, b. SPC_TPE).

$$\rho = \frac{m_{S,A} \cdot \rho_{IL}}{m_{S,A} - m_{S,IL}}, \quad (1)$$

where $m_{S,L}$ is the sample's weight in air, ρ_{IL} is the density of the liquid, $m_{S,IL}$ is the sample's weight in the liquid.

MFI (melt flow index) tests were carried out according to ISO 1133 on the matrices with a Ceast 7027.000 (Instron/Ceast (Torino, Italy)) MFI machine with a 2.16 kg load and at 135 °C (the foaming temperature) to determine the flowability of the matrices.

Tensile tests were performed on dumbbell specimens (Fig. 4) of the matrices with a Zwick Z005 (Zwick GmbH, Ulm, Germany) tensile tester machine equipped with a 5 kN load cell at room temperature, with a crosshead speed of 100 mm/min, according to ISO 527.

The peel strength of the composites was determined with a Zwick Z250 (Zwick GmbH, Ulm, Germany) tensile tester equipped with a peeling head. The 25 mm × 200 mm rectangular specimens were glued to aluminum sheets to prevent the composites from creasing. The test speed was 152 mm/min. The machine was equipped with a 250 kN load cell, and a PTFE film was inserted between the two coated layers during the consolidation process. Peel strength was calculated by dividing the average peel force by the width of the specimen.

3-point bending tests were performed on 10 mm × 80 mm specimens with a Zwick Z250 (Zwick GmbH, Ulm, Germany) tensile tester equipped with a 20 kN load cell, at room temperature, with a crosshead speed of 10 mm/min and a support distance of 64 mm according to ISO 178.

Dynamic mechanical analysis (DMA) was carried out on a TA Instruments Q800 (TA Instruments, United States) DMA tester. The temperature range was between −50 and 100 °C, the heating rate was 3 °C/min, the frequency was 1 Hz, and the amplitude was 20 μm according to ISO 6721.

The tensile tests of the composites were performed on 25 mm × 200 mm specimens at room temperature, with a Zwick Z250 (Zwick GmbH, Ulm, Germany) tensile tester equipped with a 250 kN load cell and with a crosshead speed of 5 mm/min according to ISO 527.

The composites were characterized by instrumented falling-weight impact tests performed with a Ceast Fractovis 9350 falling-weight impact testing machine (Instron, Torino, Italy) at room temperature according to ISO 6603. The total mass of the dart was 48.41 kg, the drop height was 1 m, the impact energy was 446.2 J, the diameter of the dart was 20 mm, and a 40 mm diameter supporting ring was used to clamp the 100 mm × 100 mm square specimens. The absorbed energy was divided by the thickness and the density of the composites, which gave "specific absorbed energy".

The cross-section of the composites, the structure of the MWCNT masterbatch and the MWCNT-filled matrices were examined with a JEOL JSM 6380 L A (Jeol Ltd., Tokyo, Japan) scanning electron microscope with an accelerating voltage of 10 kV and a spot size of 40 nm.

At least five specimens were tested in all cases.

3. Results and discussion

3.1. MWCNT masterbatches

As can be seen in Fig. 5, when APAO is used as the carrier of MWCNT, a far more homogeneous structure can be achieved than by using polypropylene homopolymer. The tendency to form aggregates is much lower in APAO throughout the examined area, despite the relatively high dosage of MWCNT. The nanotubes are dispersed more evenly in the APAO matrix, but dispersion is still not perfect—some areas have a lot of MWCNT, while some have none. This can be caused by the low viscosity of APAO, which can help break up MWCNT aggregates. Also, APAO was processed close to its melting temperature, as a result of which, viscosity was large enough to generate sufficient shear to disperse the nanotubes. The TPE masterbatch does not have such outstanding homogeneity as the APAO masterbatch. We found that the most typical form of CNT was the aggregates partially impregnated by the matrix.

We examined the morphology of the matrices produced with the CNT masterbatches and found that the same tendency is present as for the masterbatches: the APAO matrix provided better homogeneity due to its higher flowability. The APAO matrix had a well-dispersed structure of CNTs, while the TPE matrix showed a considerably more aggregated structure (Fig. 6).

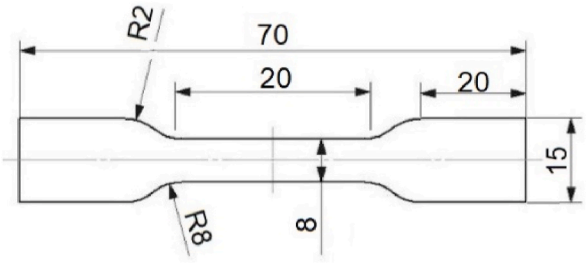

Fig. 4. The dumbbell specimen used for the tensile tests of the matrices.

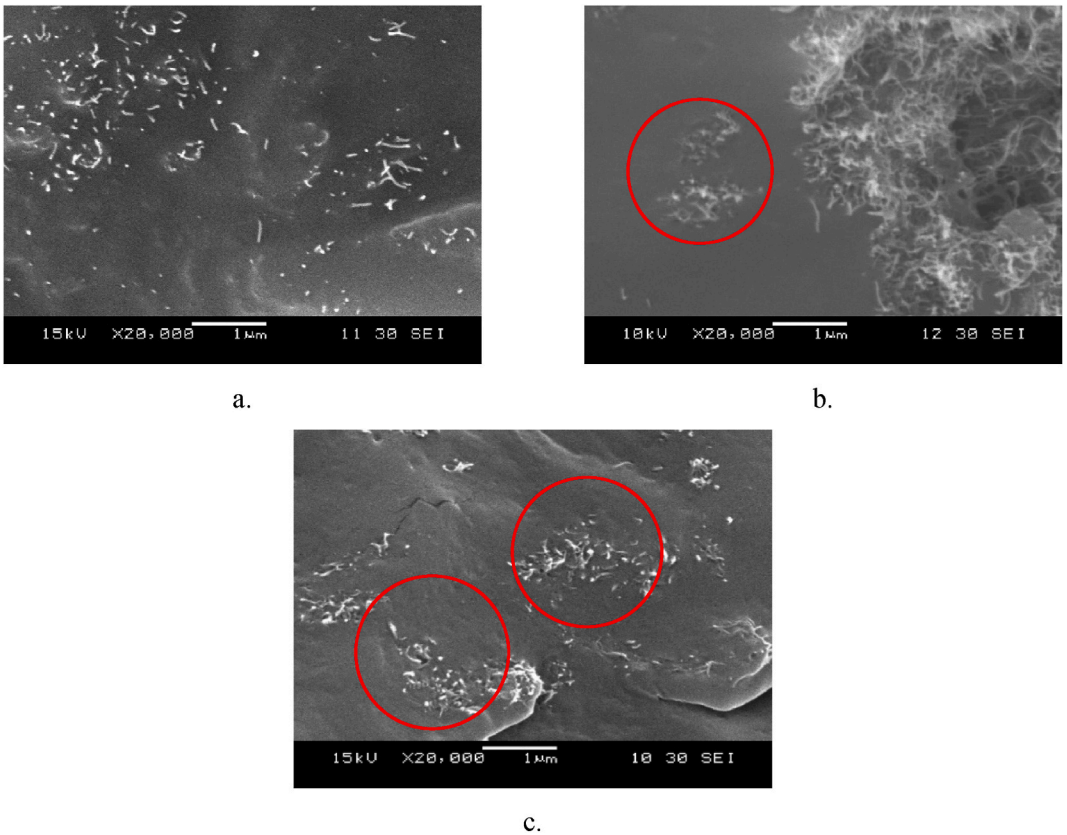

Fig. 5. SEM images of the 5 wt% MWCNT masterbatches (a. APAO; b. TPE c. PP).

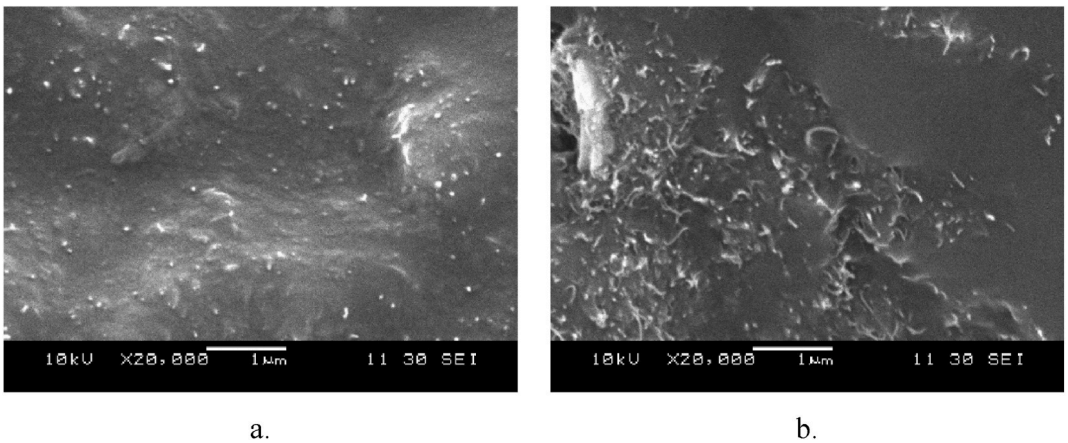

Fig. 6. SEM images of the MWCNT-filled matrices (a. APAO, b. TPE).

Table 3
Tensile properties of the matrices.

Matrix	MFI (g/10 min; 2,16 kg, 135 °C)	Tensile strength (MPa)	Young's modulus (MPa)	Elongation at break (%)
APAO	41.6 ± 5.2	3.22 ± 0.22	8.61 ± 1,25	441.9 ± 9.0
APAO/CNT	39.6 ± 7.4	3.30 ± 0.29	9.95 ± 0.95	430.6 ± 18.8
TPE	1.1 ± 0.2	15.25 ± 1.33	221.23 ± 12.95	596.1 ± 11.9
TPE/CNT	1.0 ± 0.1	18.88 ± 0.61	261.41 ± 10.57	571.7 ± 8.4

3.2. MFI of the matrixes

The MFI values (Table 3) show that APAO has a lower viscosity even at this temperature, whereas TPE has a far higher viscosity. This supports the experience that APAO can be easily processed even at 100 °C, whereas TPE was difficult to process even at 125 °C. Also, CNT slightly reduced the flow index of the matrices due to the filling.

3.3. Static tensile tests of the matrixes

The results (Fig. 7, Table 3) clearly show that TPE has considerably higher strength and elongation than APAO. Also, nanotube reinforcement successfully increased the tensile strength of the matrices.

3.4. Density of the matrices

The foaming of the matrix reduced the density of the composite in all cases (Table 4), but this reduction was more significant for the composites with an APAO matrix. It may be due to several phenomena. Firstly, APAO has lower strength and viscosity than TPE, so the microbeads were able to expand more easily. In addition, the "sticky" behavior of APAO can also cause the microbeads to be better embedded, which may also facilitate foaming. The other reason is the processing temperature of the TPE matrices: it was set to be 125 °C for both the compounding and flat film extrusion steps, which is the temperature where the microbeads start expanding. As a result, the microbeads expanded partly, but repeated heat exposure and shearing may have caused some of them to collapse, making subsequent foaming at higher temperatures less effective. This phenomenon did not occur with APAO, which is processable at 100 °C, well below the expansion temperature range of the microbeads.

The foaming of nanotube-filled matrices was less effective than that of unfilled matrices. This is due to the higher strength provided by the nanotubes.

3.5. Density of the composites

Similarly to the matrices (Section 3.4.), the density reduction of the composites with an APAO matrix is more significant than that of the composites with a TPE matrix due to the good flowability and low processing temperature of APAO (Table 5). Also, the higher strength provided by CNTs is associated with less efficient foaming.

3.6. Morphology of the composites

The SEM images (Fig. 8) show that the matrix impregnated the fabrics well in all cases, but the wetting capacity of APAO is better than that of TPE due to its better flowability.

The images of the APAO-matrix SPCs clearly show that although foaming occurred across the whole cross-section, the upper matrix layer produced far more foam cells than the lower layer. It may be because the upper layer was free to grow, whereas the lower layer was constrained by the upper layer, which caused foaming hampered. In addition, the fabric relaxes at the foaming temperature; the highly oriented tapes shrink under heat. This creates a force that can inhibit foaming. In some cases, in foam cells, the matrix and the reinforcing fabric were locally separated (circled in Fig. 9/c). In the CNT-filled composite, fewer foam cells formed due to the higher strength of the matrix.

Compared to APAO, there are fewer foam cells in the TPE matrix, which confirms the difference between the measured density values. The smearing of the matrix also hindered the examination by SEM (Fig. 10).

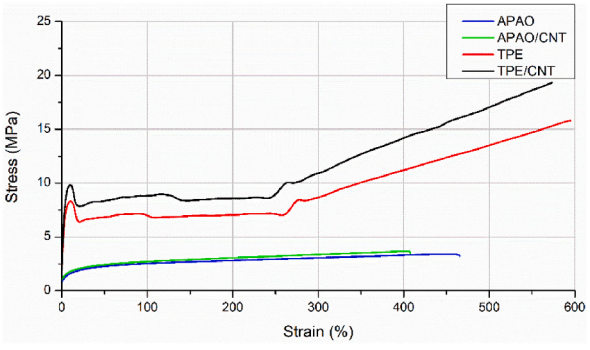

Fig. 7. Typical stress–strain curves of the matrices.

Table 4
Density of the matrices.

Matrix	Density (g/cm^3)	Matrix	Density (g/cm^3)
APAO	0.729 ± 0.006	**TPE**	0.887 ± 0.006
APAO foamed	0.462 ± 0.009	**TPE foamed**	0.723 ± 0.003
APAO/CNT	0.730 ± 0.002	**TPE/CNT**	0.890 ± 0.002
APAO/CNT foamed	0.597 ± 0.016	**TPE/CNT foamed**	0.784 ± 0.003

Table 5
Density of the composites with foamed and non-foamed matrices.

Composite	Density (g/cm^3)	Composite	Density (g/cm^3)
SPC_APAO	0.811 ± 0.006	**SPC_TPE**	0.836 ± 0.006
SPC_APAO foamed	0.487 ± 0.015	**SPC_TPE foamed**	0.729 ± 0.019
SPC_APAO/CNT	0.811 ± 0.007	**SPC_TPE/CNT**	0.832 ± 0.002
SPC_APAO/CNT foamed	0.623 ± 0.007	**SPC_TPE/CNT foamed**	0.749 ± 0.015

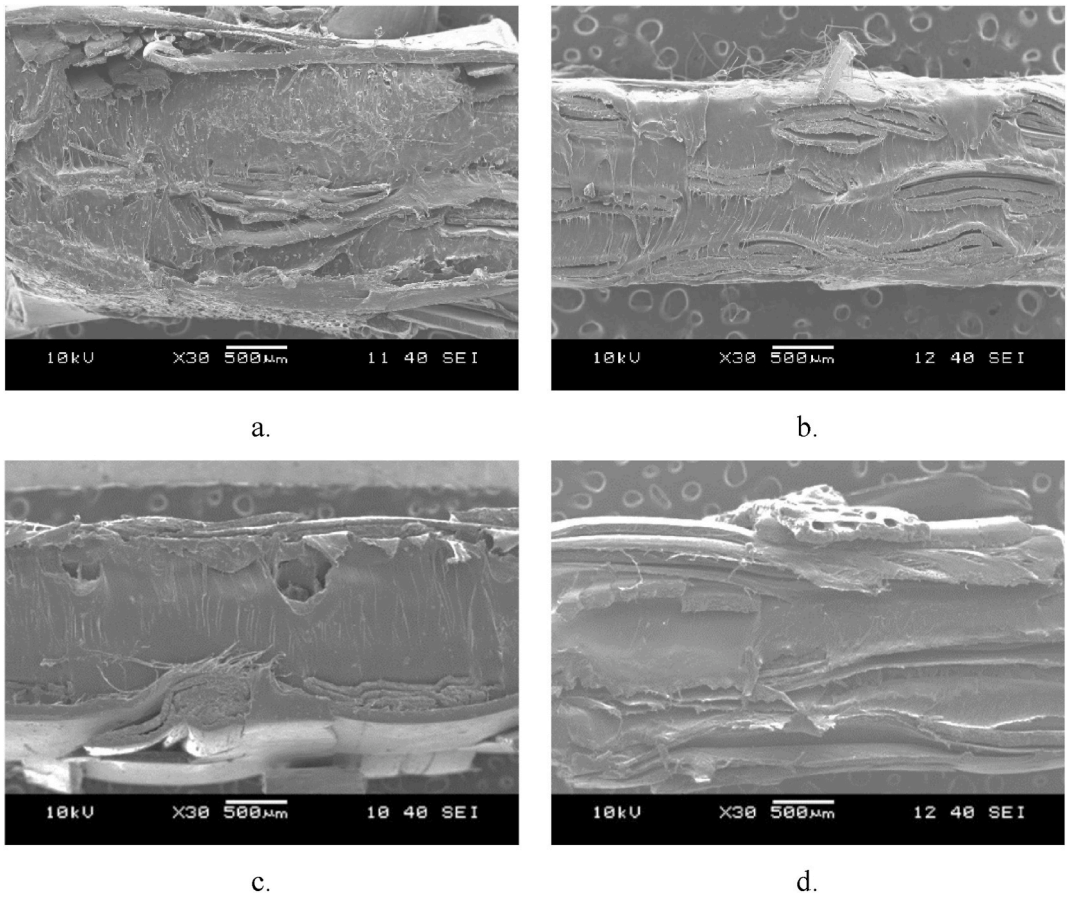

Fig. 8. SEM-images of the cross-section of the SPCs with a non-foamed matrix (a. SPC_APAO, b. SPC_APAO/CNT, c. SPC_TPE, d. SPC_TPE/CNT).

3.7. Peel tests

The composites with an APAO matrix have far higher peel strength (Table 6). APAO impregnated the fabric much better than TPE, which agrees well with the SEM images. It can be concluded that the consolidation of the APAO matrix composites is of better quality. TPE is structurally an ethylene-propylene block copolymer which, due to its longer ethylene segments, cannot adhere to the PP tapes as well as APAO, which is mainly composed of propylene repeating units. This may explain the poorer consolidation quality of the TPE composites. Foaming also reduced peel strength slightly, which may be due to the partial separation of matrix and fabric, as seen in the SEM images (Fig. 9/c).

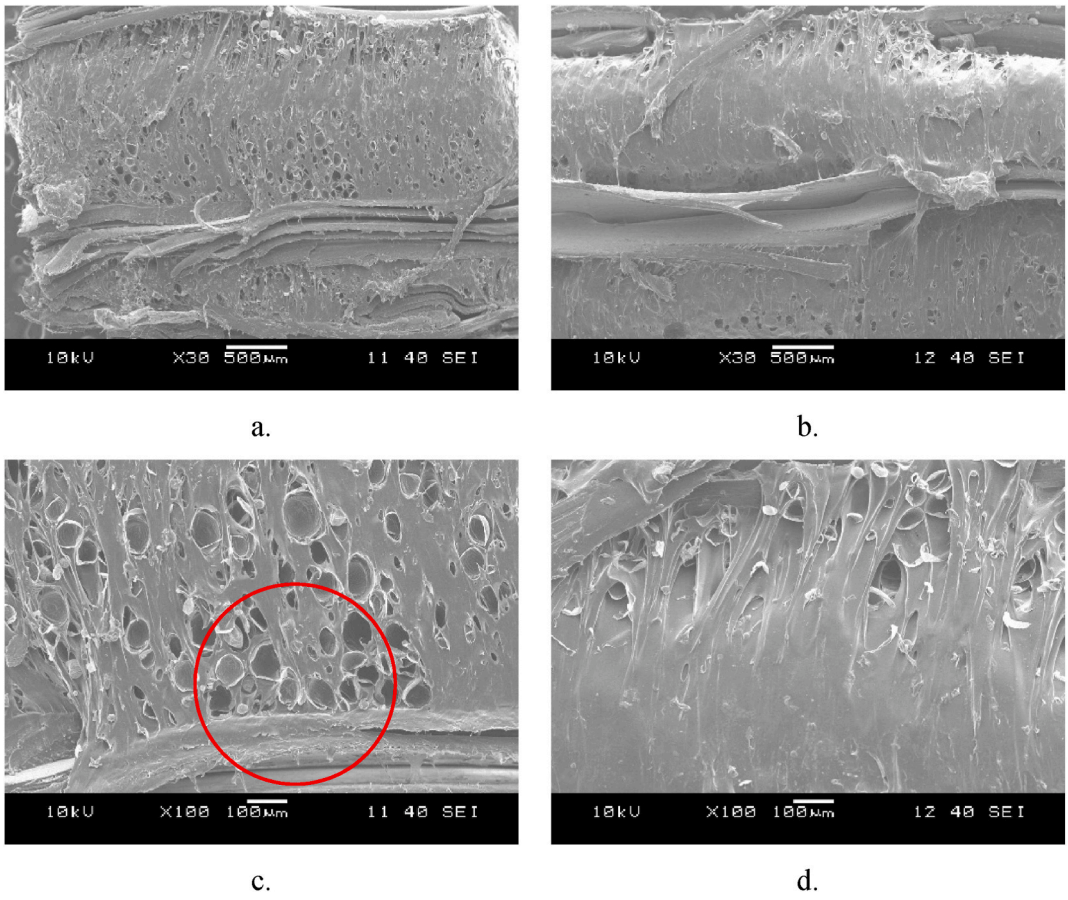

Fig. 9. SEM images of the cross-section SPCs with foamed APAO matrix (a. and c. SPC_APAO foamed, b. and d. SPC_APAO/CNT foamed).

3.8. Flexural tests of the composites

The results clearly show that the stiffness of TPE matrix composites is much higher than that of APAO matrix composites. This is due to the properties of the matrices; the strength properties of the TPE were generally better than those of the APAO. The foaming of the matrices reduced flexural stiffness, but this reduction disappeared after speciating to the density of the composites (Fig. 11, Table 7).

Furthermore, the stiffness-enhancing effect of the nano-reinforcement in the matrix is also very evident: the flexural stiffness of the composites with both the APAO and the TPE matrix significantly increased when combined with CNT, but at the same time, the composites did not become stiffer as no fracture occurred in either case.

3.9. DMA tests of the composites

T_g values (derived from storage modulus curves) decrease slightly with foaming, in agreement with the literature [27]. This decrease is more pronounced for composites with an APAO matrix, which have a more porous structure (Fig. 12, Table 8).

In addition, the DMA results also show that T_g increased slightly with the application of CNT. The explanation is that the nanotubes inhibit the movement of molecules, and therefore a slightly higher temperature is required to initiate particle movement. This is supported by the fact that this increase is greater for the more homogeneous APAO/CNT matrices than for the less homogeneous TPE/CNT matrices.

The storage moduli measured at room temperature show a similar trend to the flexural moduli. TPE has better strength properties, so it also provided higher stiffness to the composite than APAO. Foaming reduced the modulus and this reduction was far more significant for the composites with an APAO matrix, which foamed better. CNT increased the modulus—composites with CNT had higher modulus.

Several conclusions can be drawn from the shape of the DMA curves (Fig. 12/a). The modulus of all composites decreases significantly with increasing temperature, but this decrease is far more pronounced for composites with an APAO matrix, and also occurs earlier. The reason for this is the low melting temperature of the APAO matrix. Modulus loss is less significant for composites with a TPE matrix because the melt strength of TPE is also higher than that of APAO. The curves (Fig. 12/a) show the same phenomena as with bending—filling the matrix with CNTs increased the modulus in all cases, and foaming the matrix decreased it.

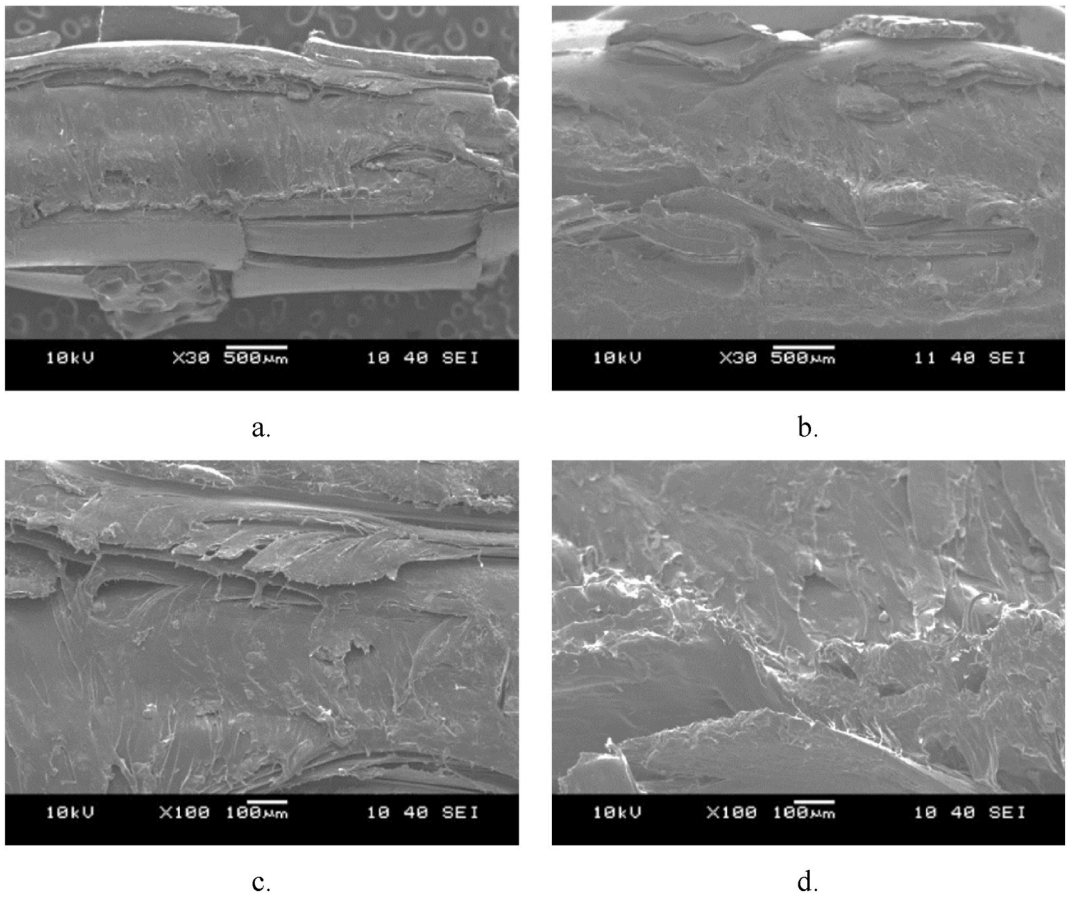

Fig. 10. SEM images of the cross-section SPCs with foamed TPE matrix (a. and c. SPC_TPE foamed, b. and d. SPC_TPE/CNT foamed).

Table 6
Peel strength of the composites.

Composite	Peel strength (N/mm)	Composite	Peel strength (N/mm)
SPC_APAO	2.69 ± 0.86	**SPC_TPE**	0.77 ± 0.05
SPC_APAO foamed	1.18 ± 0.79	**SPC_TPE foamed**	0.67 ± 0.08
SPC_APAO/CNT	2.43 ± 0.88	**SPC_TPE/CNT**	0.66 ± 0.04
SPC_APAO/CNT foamed	1.52 ± 0.42	**SPC_TPE/CNT foamed**	0.61 ± 0.06

The tan(δ) curves (Fig. 12/b) illustrate the damping behavior of the composites. It is evident that SPCs with an APAO matrix exhibit higher damping, indicating their softer nature. Additionally, foaming significantly enhances damping for both matrices, however it is much more apparent in APAO composites, due to their improved foaming capability.

3.10. Static tensile tests of the composites

The strength of the composites with an APAO matrix is generally lower than that of the composites with a TPE matrix, as the mechanical properties of APAO are inferior to those of TPE (Table 9). This trend is consistent with the trend in the flexural and DMA test results. There is also a slight difference in the shape of the tensile curves (Fig. 13): in the curves of the TPE composites, the drop after the maximum force was less abrupt and more gradual.

Although the porous structure of the foams led to a deterioration in mechanical properties, this deterioration disappeared after tensile strength was expressed relative to density; in some cases, density-relative tensile strength even improved slightly after foaming.

Reinforcing the matrix with nanotubes led to a significant increase in both the modulus and the tensile strength of the composites. The elongation at break of the composites was only slightly reduced as a result of nano-reinforcement. This may be due to the fact that the well-dispersed nanotubes were less likely to form aggregates that accelerate breakage.

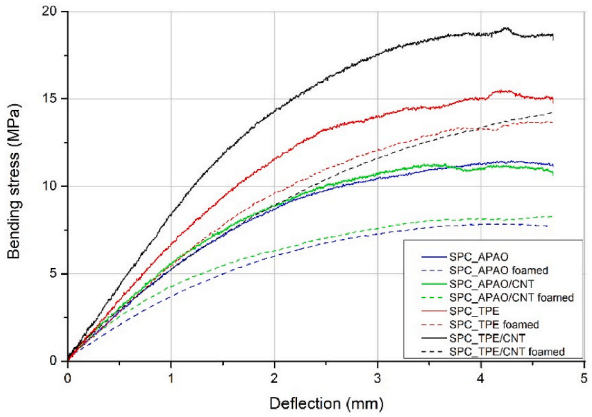

Fig. 11. Typical flexural curves of the composites.

Table 7
Results of the flexural tests.

Composite	Flexural modulus (MPa)	Flexural modulus relative to density (MPa·cm^3/g)	Limit bending stress (MPa)	Limit bending stress relative to density (MPa·cm^3/g)
SPC_APAO	542.7 ± 46.8	669.0 ± 60.9	10.9 ± 0.5	13.4 ± 0.5
SPC_APAO foamed	339.2 ± 42.5	695.1 ± 74.7	7.5 ± 0.4	15.6 ± 0.8
SPC_APAO/CNT	614.2 ± 55.7	760.7 ± 70.2	10.4 ± 0.7	12.9 ± 0.9
SPC_APAO/CNT foamed	480.2 ± 15.1	767.4 ± 20.7	8.1 ± 0.2	13.0 ± 0.1
SPC_TPE	611.7 ± 32.9	732.5 ± 37.1	14.5 ± 1.0	17.3 ± 1.2
SPC_TPE foamed	563.9 ± 34.8	774.0 ± 56.6	15.2 ± 1.4	20.8 ± 1.9
SPC_TPE/CNT	816.8 ± 17.9	981.3 ± 18.0	18.3 ± 0.8	22.0 ± 0.9
SPC_TPE/CNT foamed	580.1 ± 34.2	776.3 ± 52.3	15.1 ± 0.9	20.2 ± 1.7

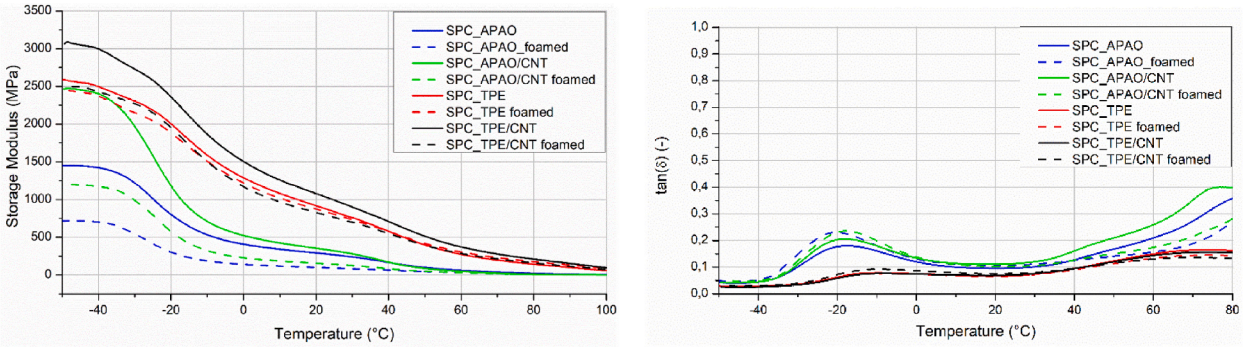

Fig. 12. DMA curves of the composites (a. Storage modulus, b. tan(δ)).

Table 8
T_g and moduli of the composites at room temperature determined by DMA.

Composite	T_g (°C)	Storage modulus at room temperature (MPa, on 23 °C)	Composite	T_g (°C)	Storage modulus at room temperature (MPa, on 23 °C)
SPC_APAO	−25.1	278	**SPC_TPE**	−16.7	872
SPC_APAO foamed	−27.1	95	**SPC_TPE foamed**	−17.0	834
SPC_APAO/CNT	−23.2	334	**SPC_TPE/CNT**	−15.9	1029
SPC_APAO/CNT foamed	−24.9	146	**SPC_TPE/CNT foamed**	−16.3	829

Table 9
Results of the static tensile tests.

Composite	Tensile modulus (MPa)	Tensile modulus relative to density (MPa·cm^3/g)	Maximum stress (MPa)	Maximum stress relative to density (MPa·cm^3/g)	Maximum strain (%)
SPC_APAO	453 ± 25	558 ± 30	43.5 ± 1.1	53.5 ± 1.4	31.8 ± 1.7
SPC_APAO foamed	265 ± 25	551 ± 5	24.5 ± 1.2	50.9 ± 4.7	24.4 ± 2.1
SPC_APAO/CNT	499 ± 20	614 ± 23	50.7 ± 4.7	62.3 ± 5.1	30.4 ± 4.1
SPC_APAO/CNT foamed	398 ± 14	635 ± 21	42.8 ± 1.6	70.9 ± 1.8	33.2 ± 2.5
SPC_TPE	934 ± 24	1120 ± 38	63.3 ± 3.2	76.1 ± 3.4	25.0 ± 2.2
SPC_TPE foamed	824 ± 25	1123 ± 39	55.8 ± 2.7	76.6 ± 5.1	25.9 ± 1.9
SPC_TPE/CNT	1034 ± 21	1243 ± 28	75.3 ± 2.1	90.5 ± 2.5	31.8 ± 2.6
SPC_TPE/CNT foamed	875 ± 23	1160 ± 36	54.8 ± 2.8	73.2 ± 4.1	30.4 ± 1.8

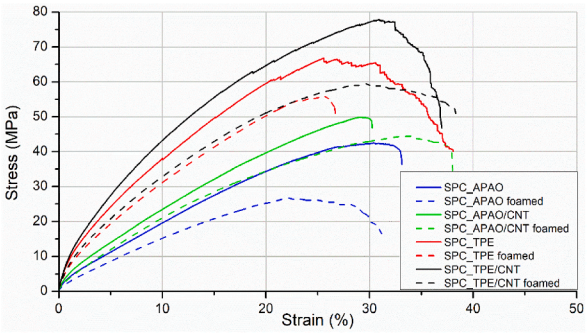

Fig. 13. Typical tensile curves of the composites.

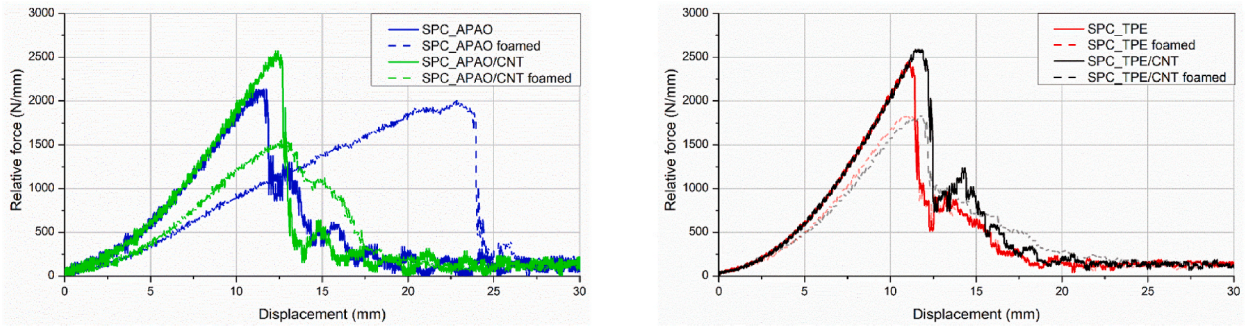

a. b.

Fig. 14. Relative force–displacement curves of the composites (a.: APAO, b.: TPE).

Table 10
Results of the falling weight tests.

Composite	Thickness (mm)	Absorbed energy (J)	Perforation energy (J/mm)	Perforation energy relative to density (J·cm^2/g)
SPC_APAO	1.80 ± 0.03	27.74 ± 1.57	15.12 ± 1.08	204.9 ± 13.1
SPC_APAO foamed	3.40 ± 0.04	73.31 ± 12.42	21.58 ± 3.82	441.4 ± 92.2
SPC_APAO/CNT	1.90 ± 0.10	28.89 ± 3.43	15.29 ± 2.56	189.2 ± 31.7
SPC_APAO/CNT foamed	2.70 ± 0.10	42.86 ± 0.61	15.86 ± 0.44	253.7 ± 31.2
SPC_TPE	1.85 ± 0.03	32.18 ± 4.45	17.36 ± 2.19	207.7 ± 26.2
SPC_TPE foamed	2.36 ± 0.26	40.72 ± 1.25	17.44 ± 2.23	239.1 ± 30.6
SPC_TPE/CNT	1.92 ± 0.03	37.11 ± 1.92	19.35 ± 1.31	232.4 ± 15.7
SPC_TPE/CNT foamed	2.68 ± 0.11	48.42 ± 0.83	18.03 ± 0.91	240.6 ± 12.2

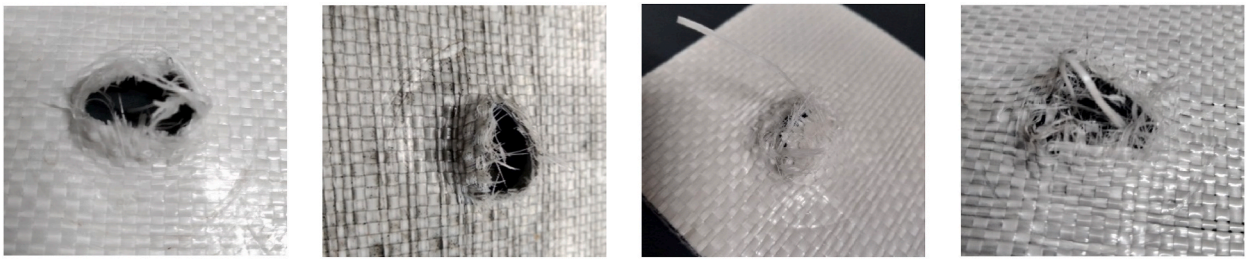

a. b. c. d.

Fig. 15. Photo images of the samples after impact test (a. SPC_APAO, b. SPC_APAO/CNT, c. SPC_TPE, d. SPC_TPE/CNT).

3.11. Instrumented falling weight tests of the composites

The effect of foaming is most apparent in the case of impact properties (Fig. 14, Table 10). In the APAO-matrix composites, perforation energy increased significantly after the matrix was foamed. This increment can be caused by the fact that the foam structure ensures greater displacement and the compression of the foam upon impact leads to this enhanced impact behavior. This tendency can be observed for absorbed energy relative to density, which means that the impact properties of the composites were increased without added weight.

As for the composites with a TPE-matrix, greater perforation energy was measured compared to the composites with an APAO matrix. This can be caused by their lower degree of consolidation, which results in tape pullout being a more characteristic failure mode, as it absorbs more energy than tape break (Fig. 15). Also, the increase in perforation energy is not as significant as with the APAO matrix. This is most likely because less foaming occurred in the TPE-based matrix.

Using nanotubes to strengthen the matrix did not result in impaired impact properties, due to the sufficient homogeneity of the MWCNTs in the matrix. The foaming process resulted in increased impact performance for the SPCs with a CNT-filled matrix. However, energy absorption decreased compared to the SPCs with an unfilled APAO matrix. This can be caused by the fact that the foaming process was inhibited by the nanotubes, as the SEM images (Fig. 9) show. As for the composites with a TPE matrix, nanotubes increased perforation energy. This may be because of their worse consolidation and tape pullouts as its consequence.

4. Conclusions

We prepared polypropylene-based single-polymer composites and examined the effects of foaming their matrix and filling them with carbon nanotubes. We used two kinds of matrices: an amorphous poly-alpha-olefin (Vestoplast 792) and a thermoplastic elastomer (Versify 2000), which was compounded with another grade of APAO (Vestoplast 703) for easier processing. Expandable microspheres in a concentration of 4 wt% were used for foaming, and multi-walled carbon nanotubes in a concentration of 0.5 wt% were used to strengthen the matrix. The composites were produced by film stacking at 120 °C and foamed at 135 °C for 20 min. Flexural tests, DMA, static tensile tests, and falling weight impact tests were performed on the composites, and their morphology was characterized with SEM images.

Foaming the matrices reduced the density of the composites. Foaming reduced the density of the APAO matrix most, because of its low processing temperature. Also, the use of CNT resulted in a slightly less reduction of density, as these matrices were stiffer.

The mechanical tests showed that although tensile and bending properties are impaired after foaming, due to the porous structure, they were not impaired and even improved in some cases when expressed relative to density. Strengthening the matrix with CNT resulted in a notable increase in these properties. The falling weight impact tests showed that foaming the matrices resulted in enhanced impact behavior—due to their porous structure, they absorbed more energy upon impact. SPCs with a TPE matrix performed better in this regard, but after foaming, the SPCs with a foamed APAO matrix outperformed SPCs with a TPE matrix. We also found that reinforcing the matrix did not worsen impact behavior, while it improved tensile properties significantly.

In this study, we have showcased a significant advancement in the field by effectively modifying the matrices of SPCs, leading to substantial enhancements in their properties, primarily impact resistance and tensile strength. These compelling findings hold great promise for the widespread adoption of SPCs as lightweight, recyclable structural materials with the ability to incorporate designable reinforcement.

Author contribution statement

Ákos Görbe: Conceived and designed the experiments, performed the experiments, analyzed and interpreted the data; wrote the paper.

László József Varga: Conceived and designed the experiments, analyzed and interpreted the data.

Tamás Bárány: Conceived and designed the experiments, analyzed and interpreted the data, Contributed reagents, materials, analysis tools or data.

Data availability statement

Data included in article/supplementary material/referenced in article.

Additional information

No additional information is available for this paper.

Declaration of competing interest

The authors declare that they have no known competing financial interests or personal relationships that could have appeared to influence the work reported in this paper.

Acknowledgments

Á. Görbe thanks for the support of the ÚNKP-21-2 New National Excellence Program of the Ministry for Innovation and Technology (ÚNKP-21-2-I-BME-227). Project no. TKP-6-6/PALY-2021 has been implemented with the support provided by the Ministry of Culture and Innovation of Hungary from the National Research, Development and Innovation Fund, financed under the TKP2021-NVA funding scheme.

References

[1] T. Czigany, Disposable or single-use plastics? Neither! Recyclable or reusable plastics, Express Polym. Lett. 14 (1) (2020) 1.
[2] H. Patil, I.P. Sudagar, R. Pandiselvam, P. Sudha, K. Boomiraj, Development and characterization of rigid packaging material using cellulose/sugarcane bagasse and natural resins, Int. J. Biol. Macromol. 246 (2023), 125641.
[3] Á. Kmetty, T. Bárány, J. Karger-Kocsis, Self-reinforced polymeric materials: a review, Prog. Polym. Sci. 35 (10) (2010) 1288–1310.
[4] T. Peijs, Composites for recyclability, Mater. Today 6 (4) (2003) 30–35.
[5] P.J.W. Hine, I. M, J. Teckoe, The hot compaction of woven polypropylene tapes, J. Mater. Sci. 33 (1998) 2725–2733.
[6] I.M. Ward, P.J. Hine, The science and technology of hot compaction, Polymer 45 (5) (2004) 1413–1427.
[7] K.J. Kim, W.-R. Yu, P. Harrison, Optimum consolidation of self-reinforced polypropylene composite and its time-dependent deformation behavior, Compos. Appl. Sci. Manuf. 39 (10) (2008) 1597–1605.
[8] J.C. Chen, C.M. Wu, F.C. Pu, C.H. Chiu, Fabrication and mechanical properties of self-reinforced poly(ethylene terephthalate) composites, Express Polym. Lett. 5 (3) (2011) 228–237.
[9] Wu Kumar, Chen Lin, Shimamura, Strain concentration of double-edge hole ductile composites in the full range of deformation by digital image correlation, Express Polym. Lett. 16 (2022) 1038–1051.
[10] T. Bárány, B. Morlin, L.M. Vas, The effect of the heat used during composite processing on the mechanical properties of fibrous reinforcement of polypropylene-based single-polymer composites, Sci. Rep. 12 (1) (2022), 20427.
[11] T. Bárány, A. Izer, T. Czigány, High performance self-reinforced polypropylene composites, Mater. Sci. Forum 537–538 (2007) 121–128.
[12] Á. Kmetty, T. Bárány, J. Karger-Kocsis, Injection moulded all-polypropylene composites composed of polypropylene fibre and polypropylene based thermoplastic elastomer, Compos. Sci. Technol. 73 (2012) 72–80.
[13] L.J. Varga, T. Bárány, Development of recyclable, lightweight polypropylene-based single polymer composites with amorphous poly-alpha-olefin matrices, Compos. Sci. Technol. (2021) 201.
[14] T. Bárány, A. Izer, T. Czigány, On consolidation of self-reinforced polypropylene composites, Plast., Rubber Compos. 35 (9) (2013) 375–379.
[15] S. Agrawal, K.K. Singh, P.K. Sarkar, Impact damage on fibre-reinforced polymer matrix composite – a review, J. Compos. Mater. 48 (3) (2013) 317–332.
[16] B. Alcock, N. Cabrera, N. Barkoula, T. Peijs, Low velocity impact performance of recyclable all-polypropylene composites, Compos. Sci. Technol. 66 (11–12) (2006) 1724–1737.
[17] G. Holden, Thermoplastic elastomers, Abstr. Pap. Am. Chem. Soc. 219 (2000). U549-U.
[18] A.S. Mohite, Y.D. Rajpurkar, A.P. More, Bridging the gap between rubbers and plastics: a review on thermoplastic polyolefin elastomers, Polym. Bull. 79 (2) (2021) 1309–1343.
[19] J.G. Drobny, Polyolefin-Based Thermoplastic Elastomers. Handbook of Thermoplastic Elastomers, 2014, pp. 209–218.
[20] F. Jakob, J. Pollmeier, S. Bisevac, H.P. Heim, Modification of self-reinforced composites (SRCs) via film stacking process, Int. Polym. Process. 37 (1) (2022) 54–69.
[21] J. Karger-Kocsis, T. Bárány, Polypropylene Handbook, Springer Nature, Switzerland, 2019.
[22] F.-L. Jin, M. Zhao, M. Park, S.-J. Park, Recent trends of foaming in polymer processing: a review, Polymers 11 (6) (2019) 953.
[23] J. Hou, G. Zhao, L. Zhang, G. Wang, B. Li, High-expansion polypropylene foam prepared in non-crystalline state and oil adsorption performance of open-cell foam, J. Colloid Interface Sci. 542 (2019) 233–242.
[24] M. Avalle, G. Belingardi, R. Montanini, Characterization of polymeric structural foams under compressive impact loading by means of energy-absorption diagram, Int. J. Impact Eng. 25 (5) (2001) 455–472.
[25] J. Wilson, Measuring impact responses of foamed polymers, J. Mech. Mater. Struct. 1 (4) (2006) 725–741.
[26] R. Bouix, P. Viot, J.-L. Lataillade, Polypropylene foam behaviour under dynamic loadings: strain rate, density and microstructure effects, Int. J. Impact Eng. 36 (2) (2009) 329–342.
[27] Á. Kmetty, K. Litauszki, Development of poly (lactide acid) foams with thermally expandable microspheres, Polymers 12 (2) (2020) 463.
[28] F.A. Soares, S.M.B. Nachtigall, Effect of chemical and physical foaming additives on the properties of PP/wood flour composites, Polym. Test. 32 (4) (2013) 640–646.
[29] Ma Yu, Phule Zhu, Zhao Wen, et al., Development of EVA/POE/SEBS microcellular foam: network structure, mechanics performance and midsole application, Express Polym. Lett. 16 (2022) 1322–1330.
[30] Z.X. Zhang, Y.M. Wang, Y. Zhao, X. Zhang, A.D. Phule, A new TPE-based foam material from EPDM/PPB blends, as a potential buffer energy-absorbing material, Express Polym. Lett. 15 (2021) 89–103.
[31] J.H. Koo, Fundamentals, Properties, and Applications of Polymer Nanocomposites, Cambridge University Press, 2016.
[32] J. Karger-Kocsis, A. Kmetty, L. Lendvai, S.X. Drakopoulos, T. Barany, Water-assisted production of thermoplastic nanocomposites: a review, Materials 8 (1) (2014) 72–95.
[33] X. Xie, Y. Mai, X. Zhou, Dispersion and alignment of carbon nanotubes in polymer matrix: a review, Mater. Sci. Eng. R Rep. 49 (4) (2005) 89–112.

[34] F. Hussain, M. Hojjati, M. Okamoto, R.E. Gorga, Polymer-matrix nanocomposites, processing, manufacturing, and application: an overview, J. Compos. Mater. 40 (17) (2006) 1511–1575.
[35] A. Kausar, Holistic analysis of nanocomposites of carbon nanotube with polypropylene, Mater. Res. Innovat. 25 (3) (2021) 186–197.
[36] D. Bikiaris, Microstructure and properties of polypropylene/carbon nanotube nanocomposites, Materials 3 (4) (2010) 2884–2946.
[37] P. Pötschke, F. Mothes, B. Krause, B. Voit, Melt-mixed PP/MWCNT composites: influence of CNT incorporation strategy and matrix viscosity on filler dispersion and electrical resistivity, Polymers 11 (2) (2019) 189.
[38] M. Mičušík, M. Omastová, I. Krupa, J. Prokeš, P. Pissis, E. Logakis, et al., A comparative study on the electrical and mechanical behaviour of multi-walled carbon nanotube composites prepared by diluting a masterbatch with various types of polypropylenes, J. Appl. Polym. Sci. 113 (4) (2009) 2536–2551.
[39] J. Zhong, A.I. Isayev, K. Huang, Influence of ultrasonic treatment in PP/CNT composites using masterbatch dilution method, Polymer 55 (7) (2014) 1745–1755.
[40] L.J. Lee, C. Zeng, X. Cao, X. Han, J. Shen, G. Xu, Polymer nanocomposite foams, Compos. Sci. Technol. 65 (15–16) (2005) 2344–2363.
[41] M. Antunes, J.I. Velasco, Multifunctional polymer foams with carbon nanoparticles, Prog. Polym. Sci. 39 (3) (2014) 486–509.
[42] Y. Yang, M.C. Gupta, K.L. Dudley, R.W. Lawrence, Conductive carbon nanofiber–polymer foam structures, Adv. Mater. 17 (16) (2005) 1999–2003.